

PROCEEDINGS OF SPIE

[SPIDigitalLibrary.org/conference-proceedings-of-spie](https://spiedigitallibrary.org/conference-proceedings-of-spie)

Mid-to-high frequency characterization of inflatable membrane optics

Choi, Heejoo, Palisoc, Art, Vikkas, Amarjiit, Esparza,
Marcos, Berkson, Joel, et al.

Heejoo Choi, Art Palisoc, Amarjiit Vikkas, Marcos Esparza, Joel Berkson, Yuzuru Takashima, Daewook Kim, Christopher K. Walker, "Mid-to-high frequency characterization of inflatable membrane optics," Proc. SPIE 11820, Astronomical Optics: Design, Manufacture, and Test of Space and Ground Systems III, 118200V (1 September 2021); doi: 10.1117/12.2594412

SPIE.

Event: SPIE Optical Engineering + Applications, 2021, San Diego, California, United States

Mid-to-high frequency characterization of inflatable membrane optics

Heejoo Choi^{a,b,*}, Art Palisoc^c, Amarjiit Pandde^a, Marcos Esparza^a, Joel Berkson^a, Yuzuru Takashima^a, Daewook Kim^{a,b,d,#}, and Christopher Walker^{d,+}

^aWyant College of Optical Sciences, University of Arizona, 1630 E. University Blvd., Tucson, AZ 85721, USA

^bLarge Binocular Telescope Observatory, University of Arizona 933 N Cherry Avenue, Tucson, AZ 85721, USA

^cL'Garde, Inc., 15181 Woodlawn Avenue, Tustin, CA 92780, USA

^dDepartment of Astronomy, University of Arizona, 933 N. Cherry Ave., Tucson, AZ 85721, USA

ABSTRACT

Inflatable membrane primary optics for space telescopes are a smart approach in the context of saving flight payload weight and volume. The Orbiting Astronomical Satellite for Investigating Stellar systems (OASIS) adopted the membrane architecture for primary optics (primary antenna, A1) to have 20 meter diameter collection area with operation bands at the terahertz frequency. The membrane is made of Kapton or Mylar film with an aluminized surface, and the balloon (transparent surface + aluminized surface) is inflated to work as the convex mirror. In order to leverage the carrying volume advantage of inflatable optics, it must be folded during launch and deployed in orbit. The thin membrane film can crumple easily when it is folded, and it should be ironed out when the telescope is deployed for observation.

We studied the microroughness and mid-to-high spatial frequency characteristics of the membrane via optical metrology to evaluate the surface properties. Because it is not of traditional shape and material, it is impossible to test with an off-the-shelf interferometer and profilometer. Moreover, the defect spatial frequency of interest is a few hundred microns to millimeters range, so the measurable field and dynamic range need to be in range of a few centimeters with microns resolution. To meet those requirements for metrology, we developed a flexible optics testbed utilizing deflectometry. The microroughness and mid-to-high frequency properties are measured with a white light interferometer and proposed methodology. The test results show that the candidate membrane is suitable for OASIS and this reliable test will guide the further design study of A1 assembly and optical system error budget.

Keywords: OASIS, space telescope, optics metrology, deflectometry, Mid-to-high frequency error, inflatable optics.

1. INTRODUCTION

The very large primary reflector (known as A1) is the key feature of OASIS. Inflatable optics has many benefits in terms of weight/volume cost per collected photon. However, the flexibility of the membrane optics has the drawback of instability and inconsistency during the fabrication process and after deployment under a harsh space environment. It is necessary to understand the optical behavior of the intrinsic membrane and/or inflatable optics to provide appropriate design requirements for the following optical components in the system and define the limit of the science objectives. [1,2]

The anticipated problematic behaviors are 1) overall shape varying, 2) microroughness of the membrane, and 3) mid-to-high spatial frequency error of inflated membrane. We have been developing various deflectometry systems, and one of those systems is adopted to measure the overall optical surface. [3] In this paper, we will introduce another deflectometry for mid-to-high frequency metrology and prove the eligibility of membrane as an optical surface.

1.1 Inflatable membrane optics

Numerous membranes have been the workhorse in space applications (Figure 1). Kapton and Teflon are the primary candidates for membrane material. For specific applications, depending on the space environment, Mylar is another good candidate. [4, 5] Doubly-aluminized Mylar, for example, is used as the inner layers of multi-layer insulation (MLI), however, it is known to degrade with long-term exposure to UV. [6] Kapton has been in use since the beginning of the space program, and Kapton-E, the thermally resistant variation, is used as the sunshields on the James Webb Space

Telescope. [7] Teflon is another good membrane candidate. One of its uses is a second surface reflector that require a low α_s/ϵ ratio (solar absorptivity/emissivity). It is beneficial for keeping the thermal environment to a low manageable level. Teflon is the most atomic oxygen resistant of the membrane optics candidates. It exhibits the lowest erosion rate against atomic oxygen which is present in low earth orbit (LEO).



Figure 1. Mylar space project (Inflatable Antenna Experiment, IAE). This test consisted of deploying and maintaining of 14 m parabolic aperture antenna in the space environment. Since the vacuum environment, $3e^{-4}$ psi is good enough to keep the surface tension. [8]

The specular membrane used to fabricate the parabolic optical mirror need to have unique properties. The first and foremost is its micro surface quality – surface roughness needs to be no more than 0.5 % RMS of science wavelength (e.g., 3 nm RMS at 600 nm object wavelength). Secondly, the material must be amenable to packaging wrinkle and crease removal upon pressurization to a stress level that is way below the membrane’s yield point. The other important characteristics include (a) low material creep, (b) retention of material integrity after exposure to UV, VUV, and ionizing radiation in a space environment, (c) retention of material/optical integrity after a few cycles of packaging and unfolding, (d) coefficient of thermal expansion (CTE) within what can be correctable by following optical system, (e) good specular properties after metallization, (f) retention of flexibility and integrity over its lifetime in a space environment, and (g) for applications in low earth orbit (LEO), resistance to atomic energy erosion. The first and second requirements belong to the mid-to-high frequency of the A1, and we will discuss them in the following.

The OASIS primary optic is a lenticular structure, Figure 2, consisting of a parabolic-like reflector membrane (metallic coating) and the symmetric canopy membrane (transparent at observation wavelength). The baseline membrane for the OASIS primary reflector optic is 12.7 μm (0.5 mils) thick Kapton with a few thousand angstroms of aluminization, whereas the canopy is black Kapton of the same thickness.



Figure 2. Prototyping 7 m diameter inflatable reflector in L’Garde site. The lenticular structure consists of the aluminized reflector and symmetric canopy.

1.2 The mid-to-high frequency error in the optical system

In traditional optics manufacturing using pitch and polishing pad with computer-controlled optical surfacing (CCOS) [9], the control and minimization of mid-to-high spatial frequency errors are highly desired in an advanced optical system. The residuals of the mid-to-high frequency error on the unit under fabrication produces background noise in the focal plane which is hard to simulate via conventional software. Because the intrinsic tool motion induces this on the unit under fabrication, all traditional large optics suffer from those errors. Many research groups, including our group, have been investigating those errors [10-13]. In order to control mid-to-high frequency, recognition of the error is an essential step, but this is a challenging metrology goal due to the large required measurable range of the testing instrument. In most optical fabrication and testing processes, various instruments are used for different frequency range coverage. For instance, in the meter-class optics process, the Fizeau interferometer (with reference reflector) covers the low-frequency surface shape, the surface profilometer measures mid-frequency, and the microscopy interferometer measures high-frequency information, as showing in figure 3.

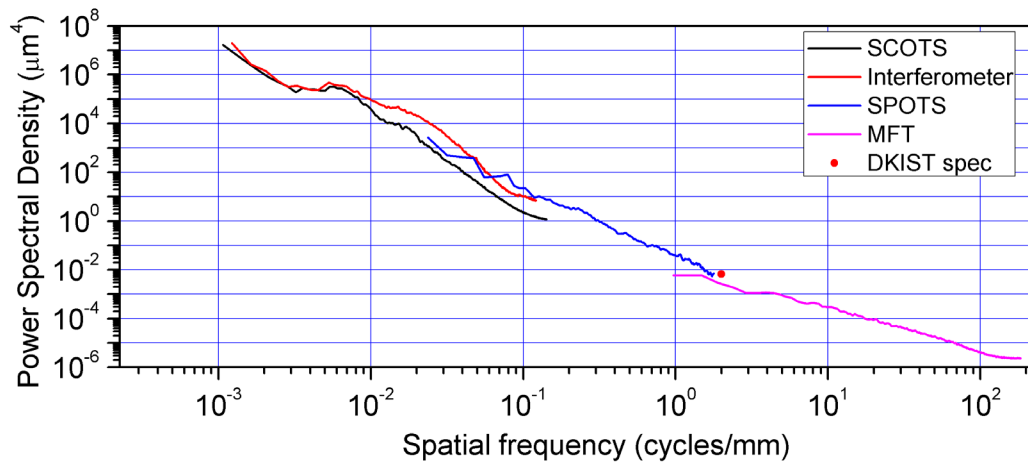


Figure 3. PSD plots from the various instrument. We have been developing and using in-house metrology system SCOTS (Software Configurable Optical Test System) and SPOTS (Slope-Measuring Portable Optical Test System) to fill the gap of the coverage of the conventional instruments. [13]

On the other hand, the OASIS A1 component is not made by tool polishing or any mechanical surface configuring approach. The films, flanges, and the gas inflation are all that can affect OASIS A1 manufacturing. Even though optics made of films do not suffer from tool mark errors, the inflated A1 still has many mid-to-high spatial frequency error sources. The mass producing mylar film sheet (polyester film) uses the roll-to-roll flow process that could create anisotropic stretch strength and cause surface wrinkle. Also, an inadequate initial surface tension of A1 assembly could be a source of the surface ruffle. In addition, the sealing boundary of the membrane using adhesion or thermal treatment are other sources of potential surface wrinkle.

Moreover, since the advantage of inflatable optics is the compact payload volume and before deployment in orbit, A1 should be folded in the payload and unfolded in space. The furl will leave a wrinkle, and all previously listed possible wrinkles sources and marks will affect optical performance as a mid-to-high frequency error.

The definition of the mid-to-high frequency errors varies regarding the target wavelength and mirror size. In the conventional meter-class optics, the range from 10^2 to 10^4 cyc/m are used for evaluation [12]. In other words, a few centimeters to the 0.1-millimeter size of wrinkle (or any defect) are the contents of the mid-to-high frequency on the A1 surface. The field of view (FoV) or measurable area of the testing instrument should be over few centimeters while retaining the spatial resolution to resolve few tens of microns of spatial structure.

1.3 Introduction to deflectometry

In 2010, the Large Optics Fabrication and Testing Group at Wyant college of optical sciences of the University of Arizona introduced the optical testing method of using a conventional PC monitor and camera with interferometer accuracy [14]. The proposed method shows the reliable optical testing result in the Giant Magellan Telescope (8.5 m class), segmented solar refractor (3 m), and refraction optic system. This method adopts the reverse-Hartman test approach and measures the

slope of the unit under test (UUT). As shown in Figure 4 (a), the surface slopes are recorded in the camera through the pixel position of the rays. The entire surface's slope is measurable as long as the monitor covers all the rays reflecting from UUT regardless of the size of the optics. The flexibility of the deflectometry layout and dynamic range has been used for various types of testing, such as simultaneous multi-segmented optics orientation testing and instantaneous optical surface measurement. [15-17] The performance of the extended deflectometry showed comparable accuracy with an interferometer. It also showed a far better accuracy than similar dynamic range instruments, as shown in Figure 4 (b).

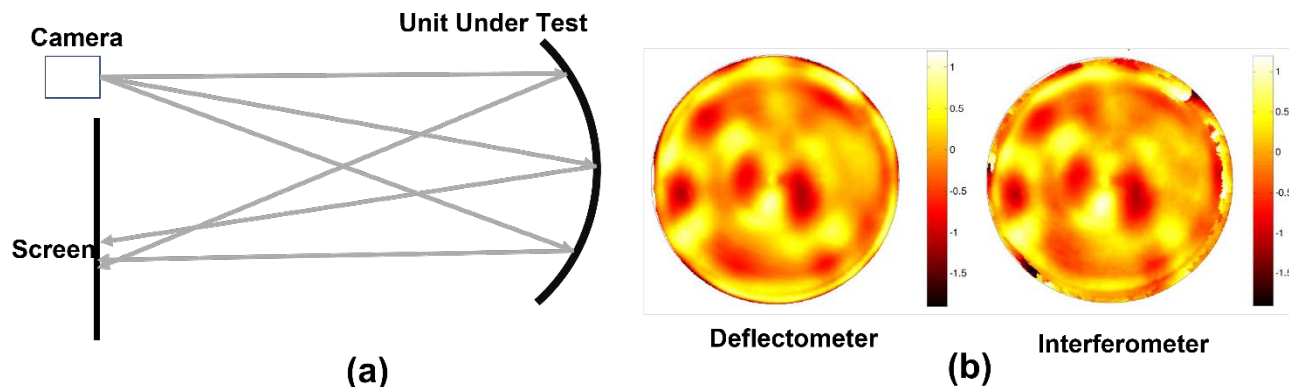


Figure 4. Schematic diagram of deflectometry and data comparison between deflectometry and interferometer [14]. (a) The ray's position on the screen gives the slope information of the UUT. Since most primary optics of telescope systems have a concave shape on primary optics, a deflectometry system can measure a meter-class mirror with a 20-30 inches PC monitor. (b) The Giant Magellan Telescope (8.5 m) mirror testing comparison. Due to the rapidly varying slope at the mirror's edge, the interferometer could not measure it smoothly.

2. EXPERIMENT

We have implemented two sets of tests for high and mid-frequency properties. The microscopic white light interferometer (WLI) with < 1.5 mm field of view (FoV) is adopted for the high-frequency property metrology. The in-house advanced deflectometry is used for a few centimeter FoV areas to evaluate mid-frequency surface property. The precision and accuracy of the in-house deflectometry are demonstrated by cross-checking with WLI.

2.1 Preparation of the inflatable samples

All membrane samples are prepared and tailored by L'Garde. The preparation of a membrane pillow sample consists of first cutting the material to the sizes needed for the application. This is followed by wiping the entire surface with isopropyl alcohol, especially in the adhesive areas. The membrane sample is kept in a dust-free environment before and after bonding to the right shape. When intended for use as an optically reflective element, care must be taken to not unnecessarily create folds and cross folds that result in permanent creases. Creases can be removed after tensioning the membrane, e.g., via pressure or edge loads, but minimizing the amount of creased areas is good practice. It also reduces the number of cross-folded areas, which may result in holes through the membrane.

The study about the adhesion is beyond the scope of this manuscript, but it is worth mentioning for the readers' information. The bonding adhesive, if not previously used, is tested on samples of the material. Peel and shear tests on bonded samples are performed to make sure the adhesive has the required strength for the intended application. Depending on whether or not the inflatable test membrane pillow will be subjected to temperature shock and/or thermal cycling, material samples for this particular test are made and subjected to the thermal environment. The bonded areas can likewise be thermally tested. For the candidate membrane materials for OASIS, thermoset and thermoplastic type adhesives can be used.



Figure 5. The photos of the pillow sample. (left) the adhesion and seamed area are taped. The red box represents the air inlet position. While optical testing, the inlet, and seamed area face downside. (middle) Air inlet. (right) Fully inflated pillow. At the middle of the pillow, the crease removal upon pressurization to a stress level below the membrane's yield point and adhesion area puncture.

The existing creases on the pillow sample are created after delivery to the University of Arizona. With preliminary inflation test in Figure 5 (c), we observed that most insignificant wrinkles are gone and few millimeter wrinkle's depths are mitigated.

2.2 Deflectometry system

The off-the-shelf PC monitor and CMOS camera are installed on 80/20 T-slot alloy frame (Figure 6). Because the UUT is a toroidal convex surface, the limited area ($3\text{ cm} \times 10\text{ cm}$, hoop \times axial) is covered by 27 inches monitor even though the camera sees almost the entire hoop. Even though we are only interested in the mid-to-high frequency structure of the sample, the testing result picks up all surface shape information. Because we calibrated this system for mid-to-high frequency testing, the low-frequency information may report a slightly deviated number from actual values. During the calibration process, the post-data processing code was developed to dismiss the low-frequency shape and was built in the data process pipeline. It is worth noting that the overall shape of the pillow (e.g., radius of curvature) is not the point of this test. From this test, we will check our system validation and understand the behavior of mid-high frequency error on the inflatable optics. The optical surface shaping test is implemented using 1 m mock of A1, and details of this test is explained in reference 3.

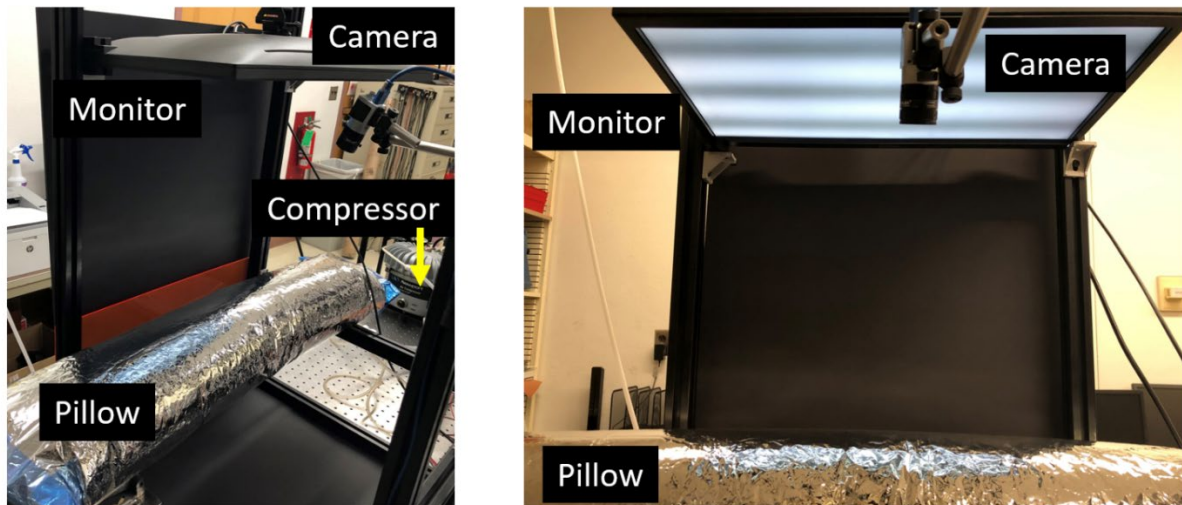


Figure 6. Deflectometry setup for pillow sample test. The compressor and regulator accommodate the inflation of the pillow.

3. DATA ANALYSIS

The microroughness ($\sim 0.8 \mu\text{m}$ spatial resolution), mid-to-high frequency structure (from 100 μm to few millimeters spatial resolution) are measured using WLI and in-house deflectometry, respectively. The WLI could measure a higher spatial resolution map, but this is unnecessary for OASIS's science spectral bandwidth (radio wave, millimeter to centimeter).

3.1 Microroughness evaluation

Three types of membranes were selected as candidate films for the OASIS primary reflector. The details of the three sheets prepared by L'Garde are in Table 1. We measured the metallic coated surface three times, and the averaged values are reported.

Table 1. Candidate film information and microroughness.

Item	Thickness (μm)	RMS (μm)	Note
Mylar	12.7 μm	0.019	0.8 \times 0.8 mm are sampled with 1024 \times 1024 pixels.
Kapton	12.7 μm	0.043	
Kapton	5 μm	0.052	

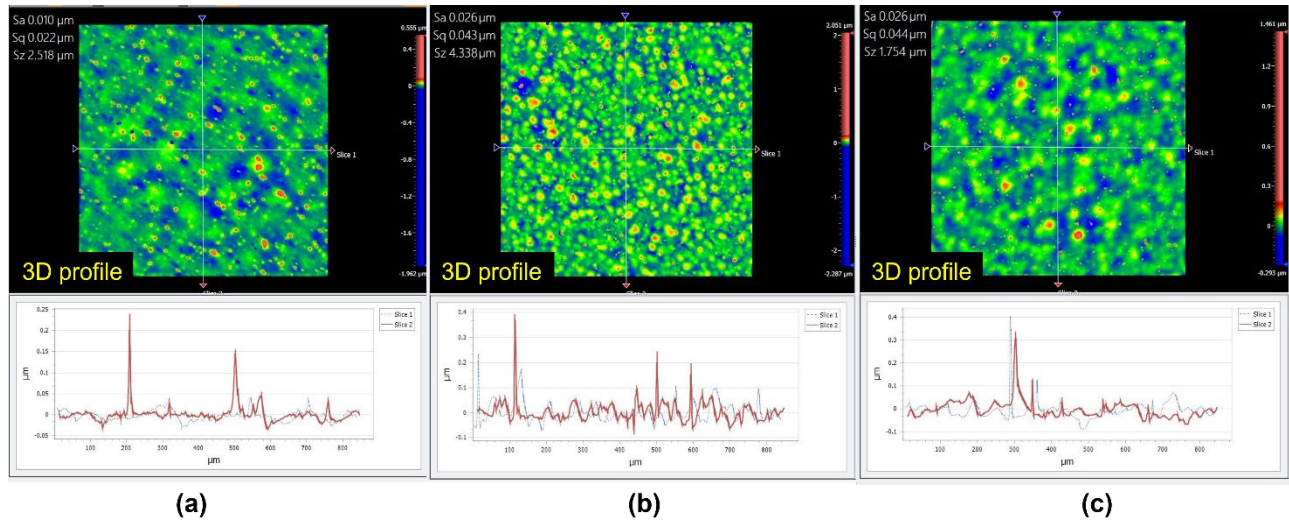


Figure 7. The microroughness test of three candidate membranes. Please be aware of the different color scales. (a) Al coated 12.7 μm Mylar, (b) Al coated 12.7 μm Kapton, (c) Al coated 5 μm Mylar. The scattered particle-like defects are the majority reason for the roughness.

The error modality of the three membranes is almost similar to the scattered particle pattern. The Kapton shows the worst roughness about 43 nm, but it is still sufficiently smooth for OASIS science goals.

3.2 Validation check of deflectometry in mid-to-high frequency measurement

Our group has been using deflectometry for various optical fabrication projects in recent decades to guide the polishing and grinding process. From those experiences, the reliability of the optical testing accuracy has been proven. The Slope-measuring Portable Optical Test System (SPOTS) [16] is the advanced deflectometry system using an auxiliary lens to measure the mid-to-high frequency of 6 m to 8 m glass optics. It is seated on the optical surface and utilizes ray trace simulation. We are not able to use this method because of 1) desire to measure the surface is inside of the lenticular structure, 2) mylar surface is not a solid, 3) it is hard to calculate the anticipated membrane surface for ray trace simulation.

Instead, we use a conventional optical layout with the limited measurable area but do further processes to extract correct information. Because this is a new approach, the validation was checked with WLI ahead of the inflated optics test.

The piece of Mylar membrane (Figure 8) is attached on top of an aluminum block with deliberately sandwiched granular. The four granular are measured with both instruments and the results are presented in Figure 9.

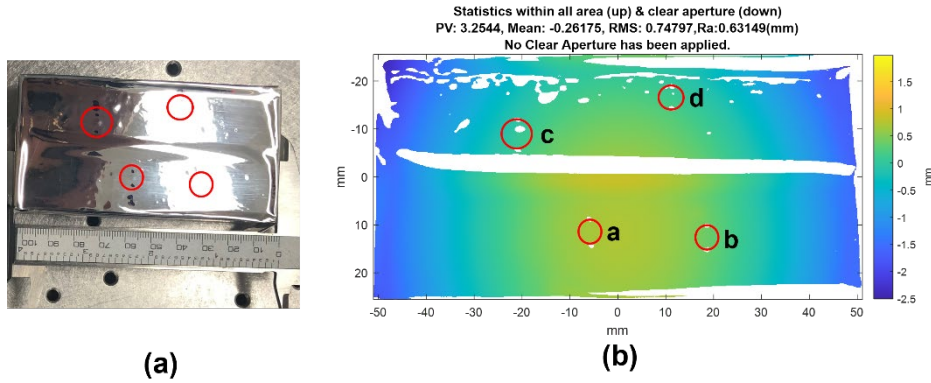


Figure 8. The sample for crosschecking and the measured surface using normal mode deflectometry. (a) The fiducials are marked at the object particle positions. (b) The surface map from the normal mode deflectometry. The not-measurable area (white region) occurred due to the too stiff slope on the surface.

After the post-process of the surface map in Figure 8 (b), the height and spot shapes are clearly shown in figure 9. The white region in Figure 8 (c) and (d) are occurred from a too steep slope. Based on the result, our approach can measure the height and shape of the few millimeters structure that is considered as mid-to-high frequency information.

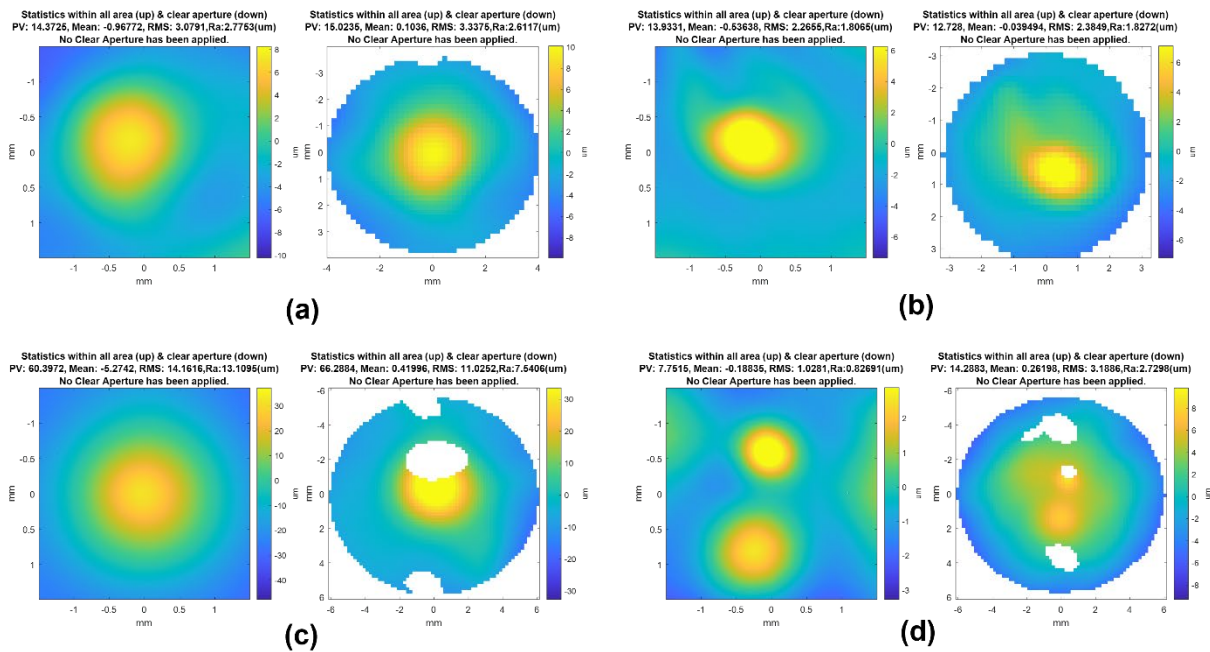


Figure 9. The comparison of WLI and deflectometry. Left surface maps are WLI, and right maps are deflectometry. We measured four areas where the particles are located. Please be aware of the x and y scale.

3.3 Deflectometry test of mid-to-high frequency for inflated membrane

We set the region of interest on the UUT and continuously measured and reported the statistics. Deflectometry measured 3 cm × 10 cm, we cropped the data to show a reasonable color scale range with various wrinkle shape and depth. The pressure was controlled with a regulator, which needed continuous inflating due to the slight leakage of the pillow sample. The surface map was taking when the pressure is stable at target pressure. We applied a consistent color scale for a coherent height-color scale. As shown in Figure 10, as we raised the pressure of the pillow, the millimeter scale crease is mitigated, and the roughness is reduced.

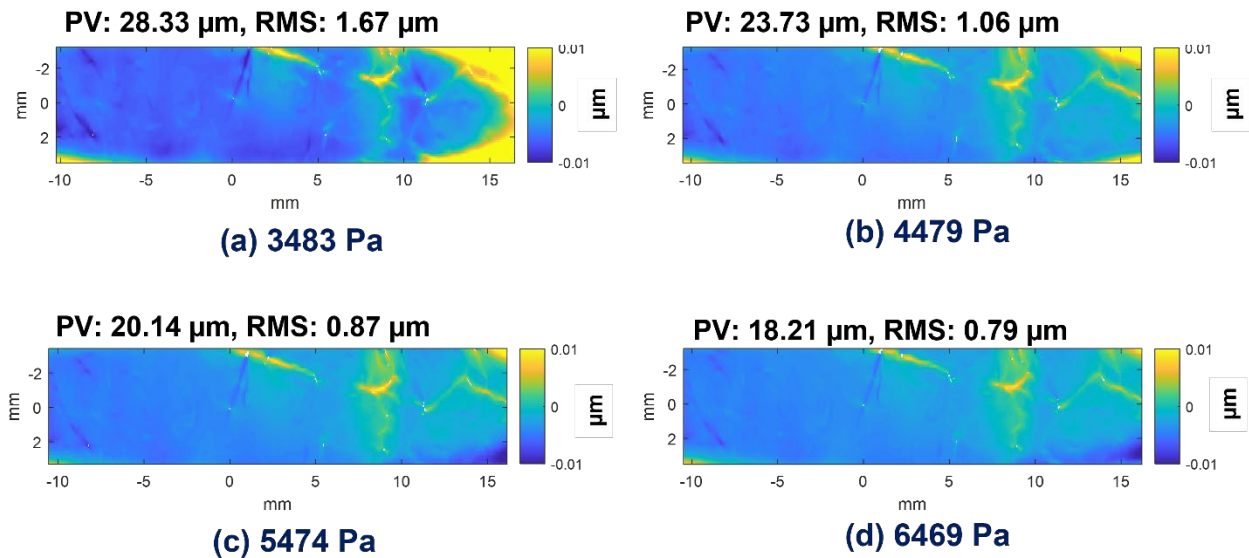


Figure 10. Mid-to-high surface shape change with pressure control. As the pressure is raised, the surface is getting smoother. The right-side corner edge contributes a big error value, but it is also decreasing. The areas in these plots are selected to show the various spatial frequency error, so the RMS error is over the requirements for OASIS. But the real OASIS A1 will be handled carefully and won't have the wrinkles shown in this plot.

Due to the pillow structure, the stress distributions of the pillow surface are different in the direction of the hoop and axial as the below equations.

$$\sigma_A = \frac{pR}{2t} \text{ and } \sigma_H = \frac{pR}{t} \quad (1)$$

The variable in the above equation, p , R , and t , corresponds to pressure, radius of the pillow, and thickness of the membrane, respectively. The σ_A is the stress of axial direction, and σ_H is the stress of the hoop direction. Based on the mathematical interpretation, the hoop directional mitigation speed will be twice the axial crease. The individual post-process of the orthogonal direction will provide the essential pressure to treat the various depth of creases, and it will guide the pressure unit design and membrane handling/seaming plan to minimize the defect.

4. CONCLUSION

The inflatable optics of OASIS is a game-changer for large-aperture space telescopes, and the size of 20 m aperture A1 will be an unprecedented optical system in space. The membrane surface of A1 shows that the optical performance of in mid-to-high frequency range is evaluated in this paper. The results confirmed that it is a sufficient optical specification of microroughness for our target wavelength. Moreover, it comes out that the claimed metrology approach is able to measure the essential information in an interesting spatial frequency range (from a few hundred microns to millimeters). The

capability of the proposed method will provide the guideline for the error budget of the A1 assembly and the requirement of the following optical system's error.

ACKNOWLEDGEMENTS

The authors would like to acknowledge the II-VI Foundation Block-Gift, Technology Research Initiative Fund Optics/Imaging Program, and Friends of Tucson Optics Endowed Scholarships in Optical Sciences for helping support the metrology research conducted in the LOFT group.

REFERENCES

- [1] Jonathan W. Arenberg, Michael Nolan, Michael Petach, Art Palisoc, Gordon Chin, Yuzuru Takashima, Daewook Kim, Christopher K. Walker. "Orbiting Astronomical Satellite for Investigating Stellar Systems (OASIS) observatory design." Proc. SPIE, Astronomical Optics: Design, Manufacture, and Test of Space and Ground Systems III, 11820-30, (Aug, 2021).
- [2] Jonathan W. Arenberg, John Pohner, George Harpole, Ariane Walker-Horne, Michael Nolan, Michael Nolan, Yuzuru Takashima, Gordon Veal, Art Palisoc, Daewook Kim, Christopher K. Walker. "Design and performance of the Orbiting Astronomical Satellite for Investigating Stellar Systems (OASIS)." Proc. SPIE, Astronomical Optics: Design, Manufacture, and Test of Space and Ground Systems III, 11820-31, (Aug, 2021).
- [3] Henry Quach, Marcos Esparza, Hyukmo Kang, Aman Chandra, Heejoo Choi, Joel Berkson, Karlene Karrfalt, Siddhartha Sirsi, Yuzuru Takashima, Art Palisoc, Jonathan W. Arenberg, Kristy Gogick Marshall, Christopher S. Glynn, Sean M. Godinez, Marcos Tafoya, Christopher Walker, Christian Drouet d'Aubigny, Daewook Kim, "Deflectometry-Based Thermal Vacuum Testing for a Pneumatic Terahertz Antenna" Proc. SPIE, Astronomical Optics: Design, Manufacture, and Test of Space and Ground Systems III, 11820-34, (Aug, 2021).
- [4] GSFC, NASA. "Preliminary Mission Report Spartan 207/Inflatable Antenna Experiment Flown on STS-77, Spartan Project Code 740.1, 1997."
- [5] Freeland, R. E., G. D. Bilyeu, G. R. Veal, M. D. Steiner, and D. E. Carson. "Large inflatable deployable antenna flight experiment results." *Acta Astronautica* 41, no. 4-10 (1997): 267-277.
- [6] Dever, Joyce A. Low earth orbital atomic oxygen and ultraviolet radiation effects on polymers. No. N-91-19294. National Aeronautics and Space Administration, 1991.
- [7] Waldie, Dean, and Larry Gilman. "Technology development for large deployable sunshield to achieve cryogenic environment." In *Space 2004 Conference and Exhibit*, p. 5987. 2004.
- [8] Wada, Ben, and Michael Lou. "Pre-flight validation of gossamer structures." In *43rd AIAA/ASME/ASCE/AHS/ASC Structures, Structural Dynamics, and Materials Conference*, p. 1373. 2003.
- [9] Kim, Dae Wook, Won Hyun Park, Hyun Kyoung An, and James H. Burge. "Parametric smoothing model for visco-elastic polishing tools." *Optics express* 18, no. 21 (2010): 22515-22526.
- [10] Del Hoyo, Javier, Heejoo Choi, James H. Burge, Geon-Hee Kim, and Dae Wook Kim. "Experimental power spectral density analysis for mid-to high-spatial frequency surface error control." *Applied optics* 56, no. 18 (2017): 5258-5267.
- [11] Kim, Dae Wook, Hubert M. Martin, and James H. Burge. "Control of mid-spatial-frequency errors for large steep aspheric surfaces." In *Optical Fabrication and Testing*, pp. OM4D-1. Optical Society of America, 2012.
- [12] Aikens, David M., Jessica E. DeGroot, and Richard N. Youngworth. "Specification and control of mid-spatial frequency wavefront errors in optical systems." In *Optical Fabrication and Testing*, p. OTuA1. Optical Society of America, 2008.
- [13] Kim, Dae Wook, Chang-jin Oh, Andrew Lowman, Greg A. Smith, Maham Aftab, and James H. Burge. "Manufacturing of super-polished large aspheric/freeform optics." In *Advances in Optical and Mechanical Technologies for Telescopes and Instrumentation II*, vol. 9912, p. 99120F. International Society for Optics and Photonics, 2016.
- [14] Su, Peng, Robert E. Parks, Lirong Wang, Roger P. Angel, and James H. Burge. "Software configurable optical test system: a computerized reverse Hartmann test." *Applied optics* 49, no. 23 (2010): 4404-4412.

- [15] Choi, Heejoo, Isaac Trumper, Matthew Dubin, Wenchuan Zhao, and Dae Wook Kim. "Simultaneous multi-segmented mirror orientation test system using a digital aperture based on sheared Fourier analysis." *Optics express* 25, no. 15 (2017): 18152-18164.
- [16] Maldonado, Alejandro V., Peng Su, and James H. Burge. "Development of a portable deflectometry system for high spatial resolution surface measurements." *Applied optics* 53, no. 18 (2014): 4023-4032.
- [17] Trumper, Isaac, Heejoo Choi, and Dae Wook Kim. "Instantaneous phase shifting deflectometry." *Optics express* 24, no. 24 (2016): 27993-28007.